



University of Stuttgart
Germany

EXPERIMENTAL
INVESTIGATIONS ON THE
HEAT TRANSFER
CHARACTERISTICS OF
SUPERCRITICAL CO₂ IN
HEATED HORIZONTAL
PIPES

Konstantinos Theologou*
Rainer Mertz
Eckart Laurien
Jörg Starflinger

IKF

Outline

- Motivation and aims
- Experimental setup
- Data reduction
- Results
- Summary & Conclusion

Motivation

since Fukushima the decay heat removal became a main part in the reactor safety research

STARTING POSITION

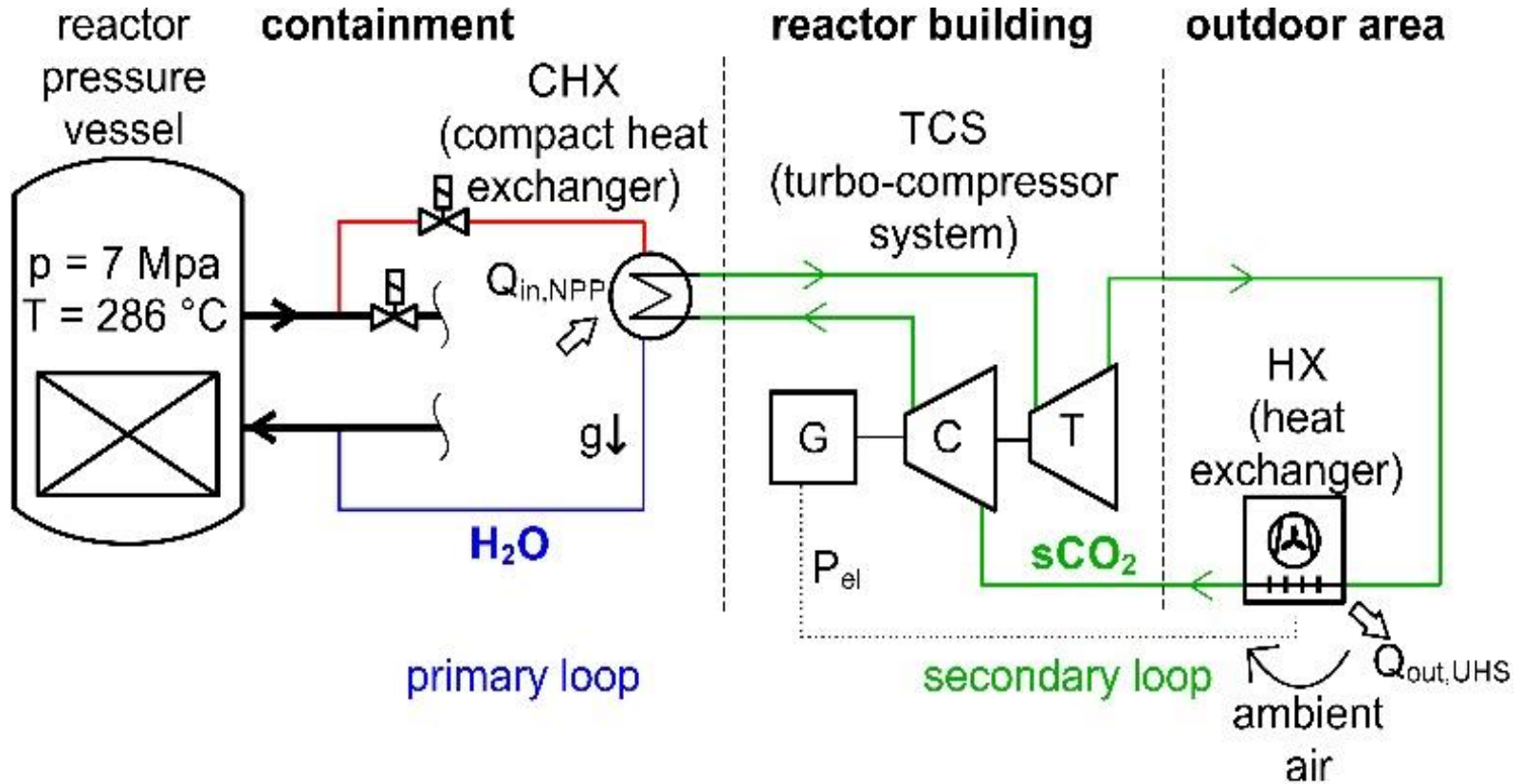
- decay heat must be transferred from the reactor core to the environment
- possibility that active safety system does not work
- passive safety systems and redundant heat sinks of new reactor concepts can not be retrofitted into existing plants

NEW CONCEPT

- sCO₂-operated decay heat removal system based on a Brayton cycle
- works without power grid connection, is self-sufficient and starts automatically
- compact system, can be retrofitted into existing power plants

Motivation

new concept – sCO₂-operated decay heat removal system



Aims

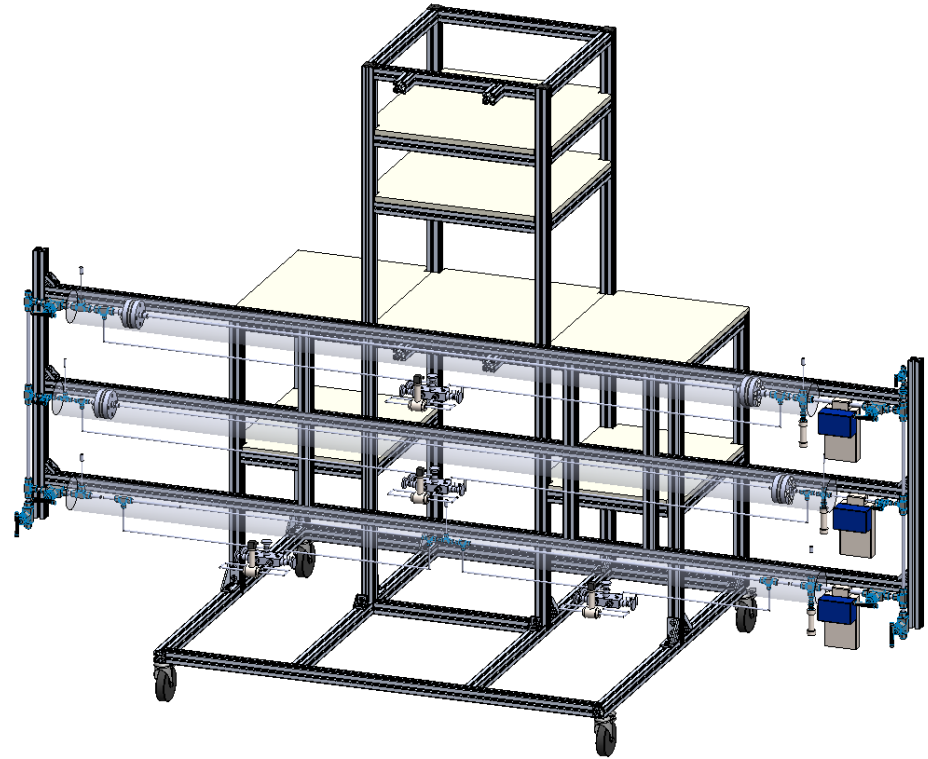
before implementing such a system accurate system simulations are needed

- the system was simulated with the German thermal hydraulic system code ATHLET by Venker but the results of the simulation show large deviations to the existing experimental data near the critical point
- ATHLET uses heat transfer and pressure loss correlations, so experimental data is needed to validate these correlations

In this presentation:

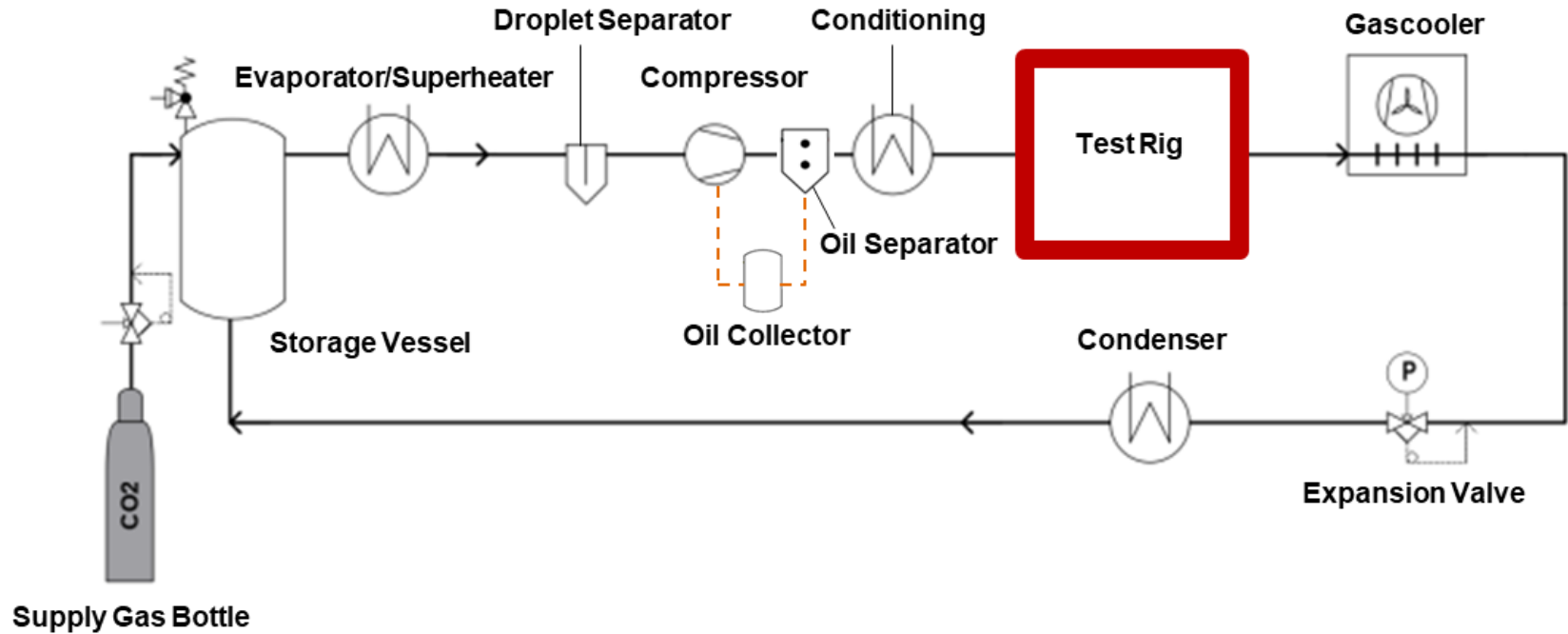
→ investigation on the heat transfer characteristics of sCO₂ in heated horizontal pipes

Experimental setup overview



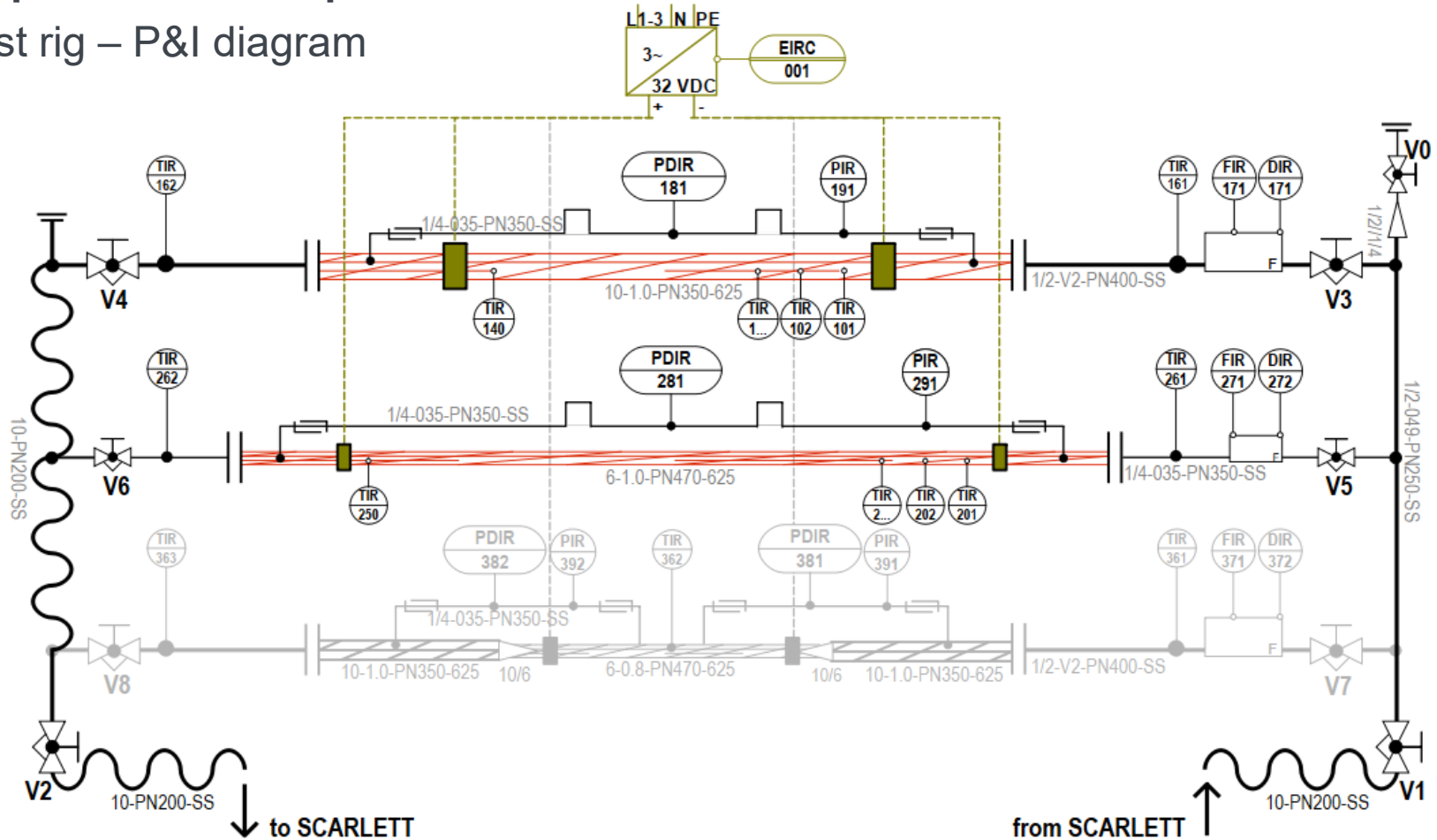
Experimental setup

test facility SCARLETT



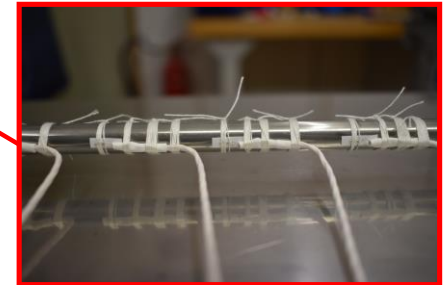
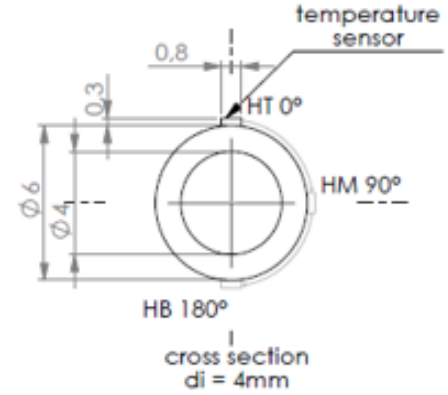
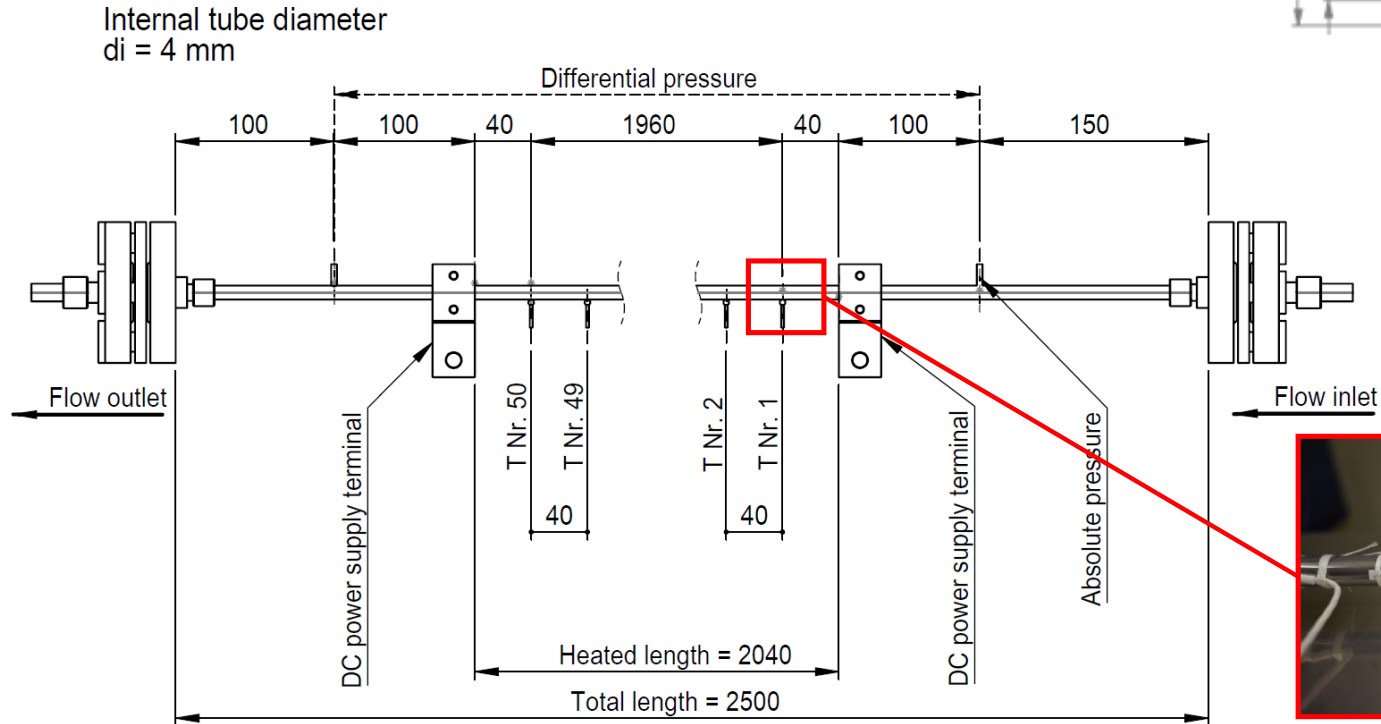
Experimental setup

test rig – P&I diagram



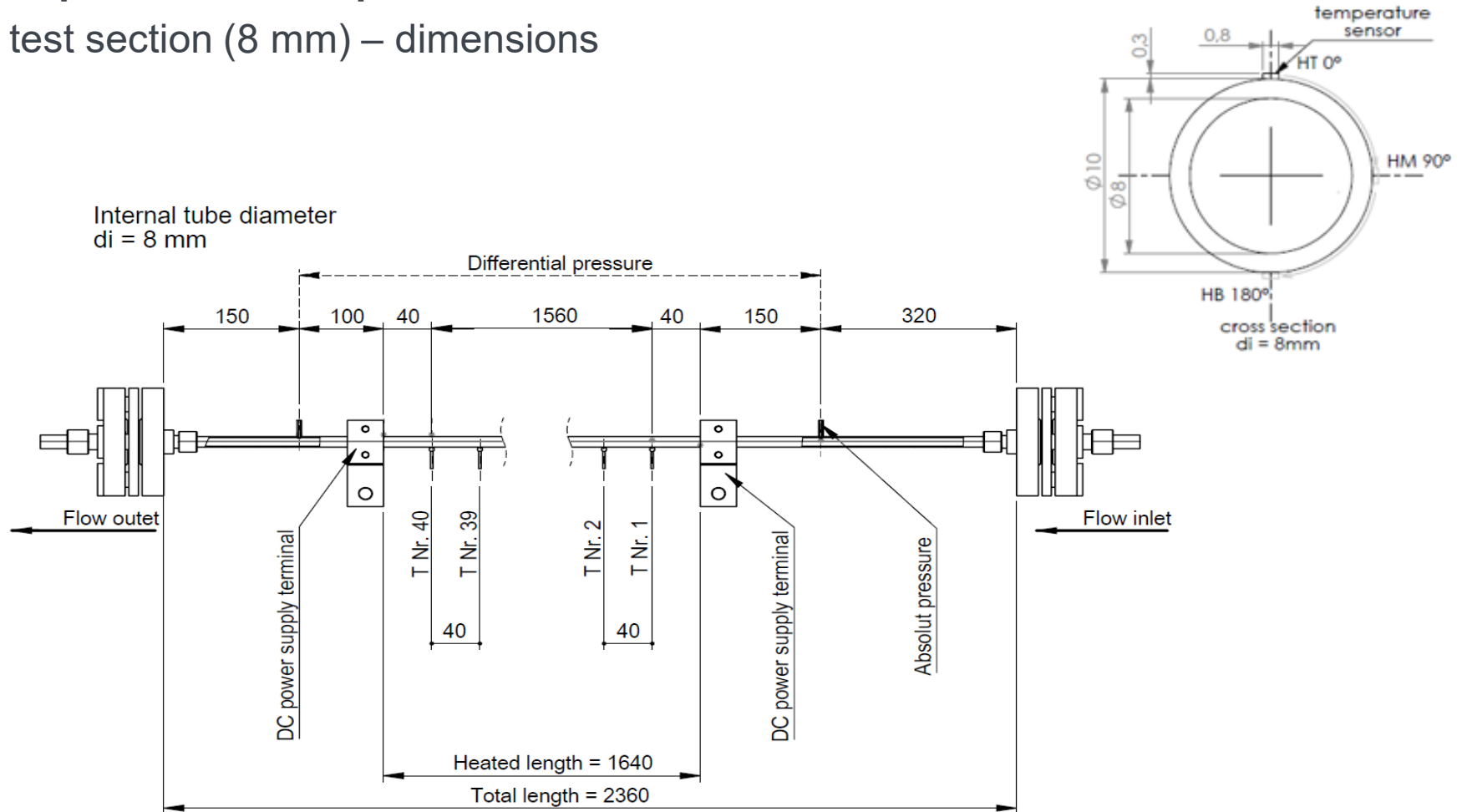
Experimental setup

test section (4 mm) – dimensions



Experimental setup

test section (8 mm) – dimensions



Data reduction

measured parameter

$$\dot{m}; T_{b,in}; T_{b,out}; T_{sur,x}; p_{in}; p_{diff}; I; V$$

1. Calculation of heat flow

$$|\dot{Q}_1| = |\dot{Q}_2| = \dot{Q} \text{ [W]}$$

$$\dot{Q}_1 = \dot{m}_1 * [h_1''(\vartheta'', p'') - h_1'(\vartheta', p')] \text{ [W]}$$

2. Calculation of heat flux

$$\dot{Q}_2 = P_{el} = U * I \text{ [W]}$$

$$\dot{q}_{tube} = \frac{\dot{Q}_2}{A_{i,sur}} = \frac{U * I}{\pi * d_i * L_h} \left[\frac{\text{W}}{\text{m}^2} \right]$$

3. Calculation of the bulk enthalpy

$$i_{b,x} = i'_b + \left(\frac{L_x}{L_h} \right) * \frac{\dot{Q}_2}{\dot{m}} \left[\frac{\text{kJ}}{\text{kg}} \right]$$

4. Calculation of bulk fluid temperature

$$T_{b,x} = f(i_{b,x}, p_x) \text{ [}^\circ\text{C]} \text{ with } p_x = p_{in} - \frac{p_{diff}}{L_h} * L_x \text{ [bar]}$$

5. Calculation of volumetric heat flux

$$\dot{q}_V = \frac{\dot{Q}_2}{\frac{\pi}{4}(d_o^2 - d_i^2) * L_h} \left[\frac{\text{W}}{\text{m}^3} \right]$$

6. Calculation of inner wall temperature

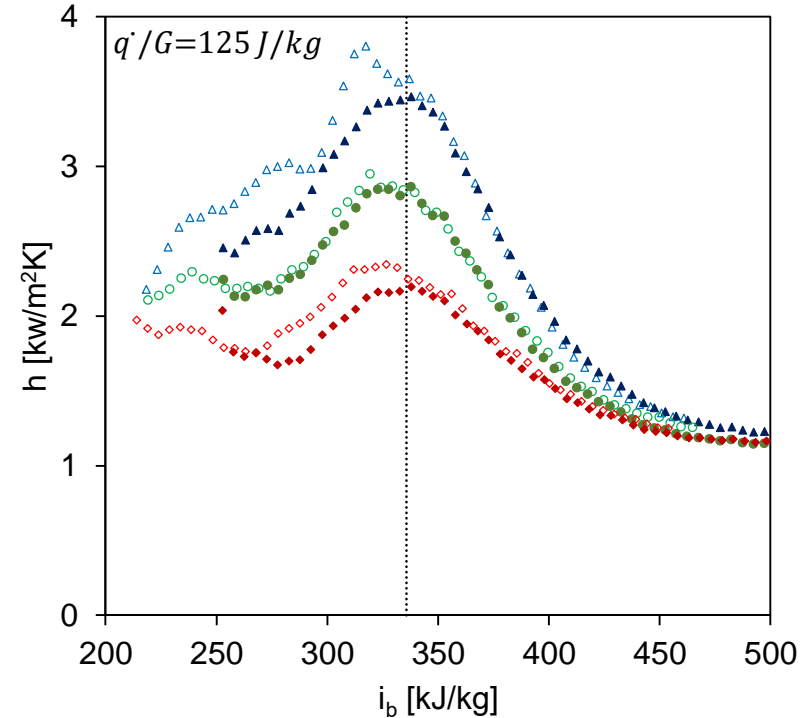
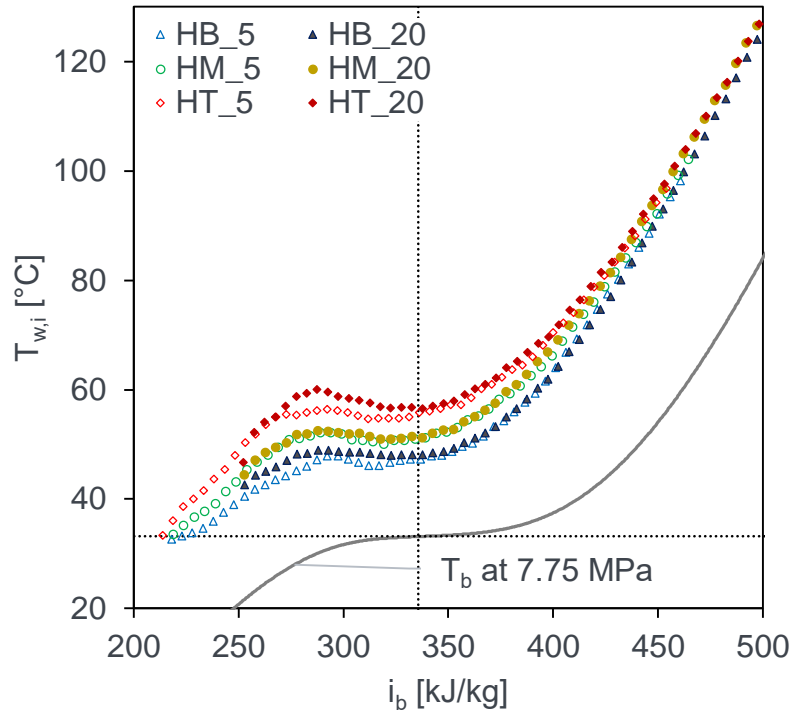
$$T_{W,i} = T_{W,o} + \frac{q_V}{4\lambda_w} \left[\left(\frac{d_o}{2} \right)^2 - \left(\frac{d_i}{2} \right)^2 \right] - \frac{q_V}{2\lambda_w} \left(\frac{d_o}{2} \right)^2 * \ln \left(\frac{d_o}{d_i} \right) \text{ [}^\circ\text{C]}$$

7. Calculation of heat transfer coefficient

$$h_x = \frac{\dot{q}}{T_{W,x} - T_{b,x}} \left[\frac{\text{W}}{\text{m}^2\text{K}} \right]$$

Results

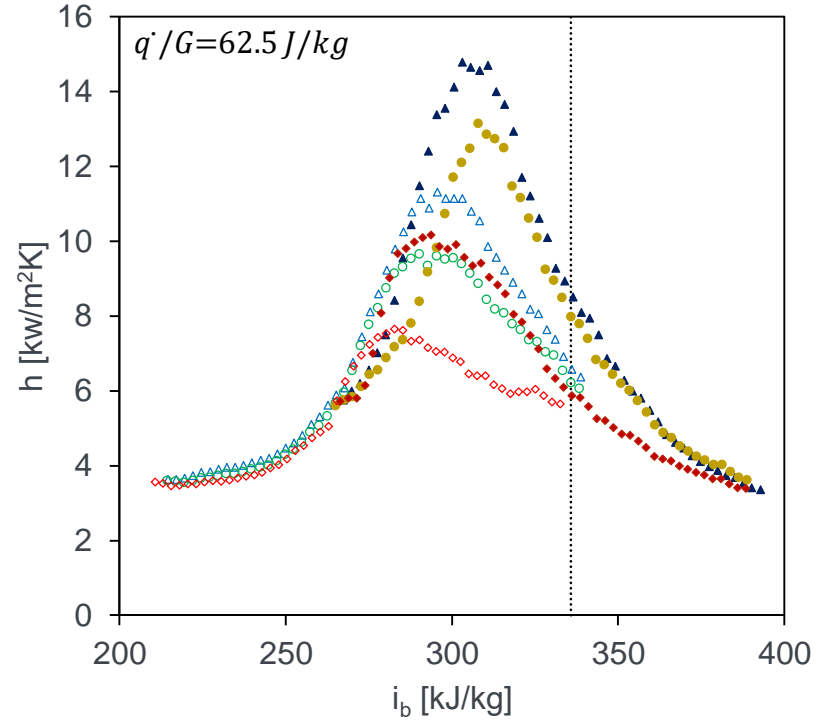
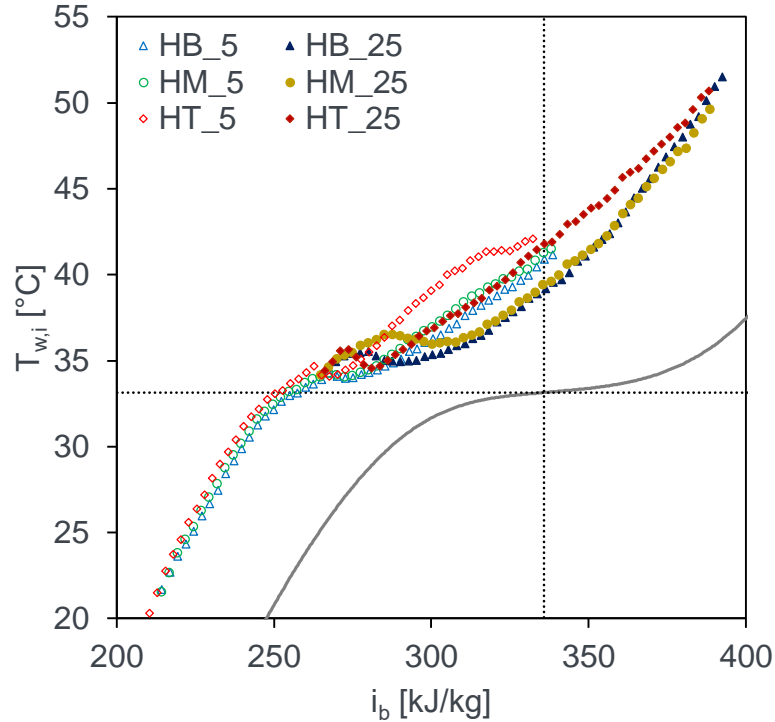
1st test series – $d_i = 4 \text{ mm}$; $p = 7.75 \text{ MPa}$, $G = 400 \text{ kg/m}^2\text{s}$; $\dot{q} = 50 \text{ kW/m}^2$



- stable temperature stratification in an enthalpy range of 220 – 450 kJ/kg
- max. temperature difference between top and bottom surface approx. 10 K

Results

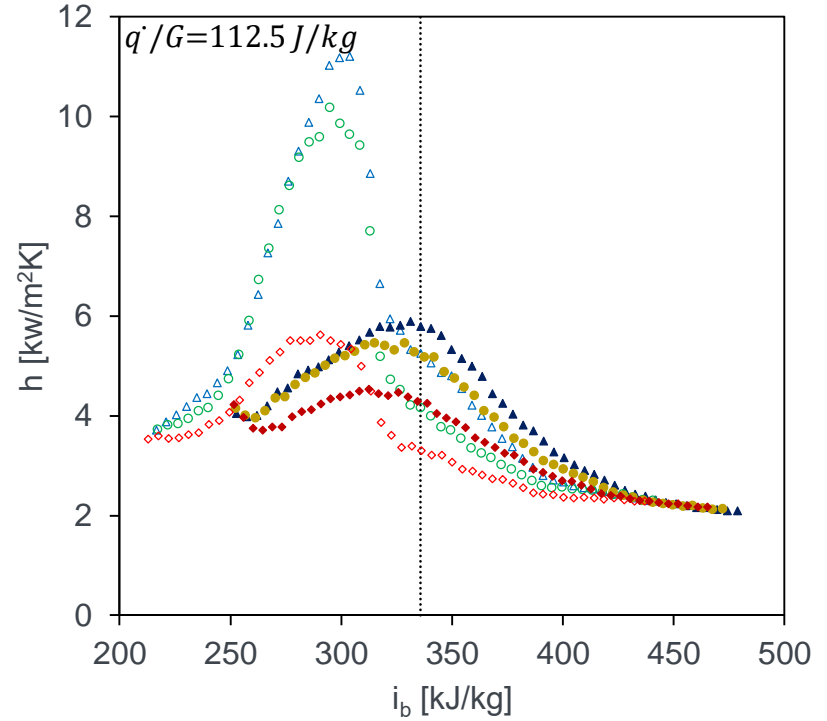
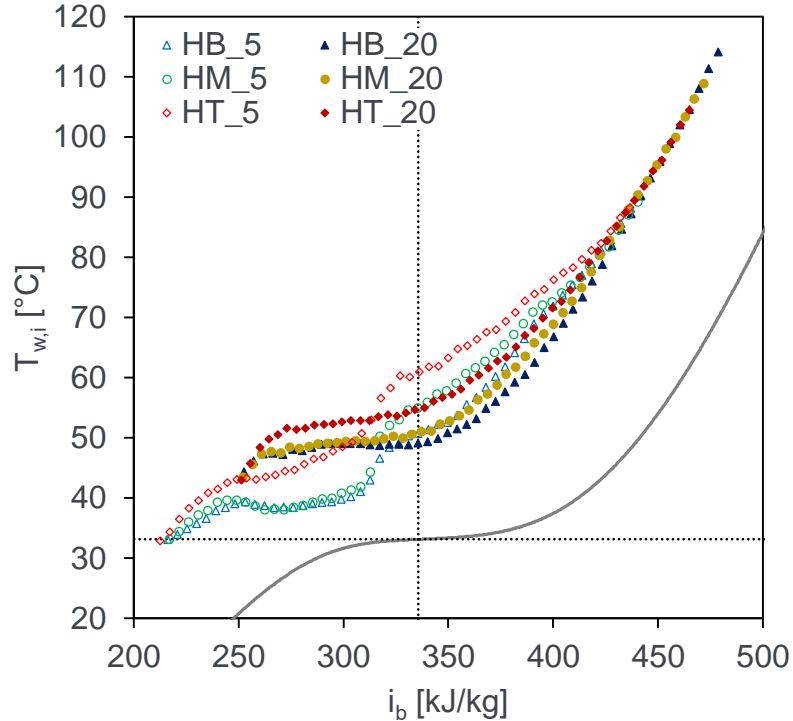
2nd test series – $d_i = 4 \text{ mm}$; $p = 7.75 \text{ MPa}$, $G = 800 \text{ kg/m}^2\text{s}$; $\dot{q} = 50 \text{ kW/m}^2$



- no clear temperature stratification
- temperature values converge after an enthalpy of approx. 390 kJ/kg

Results

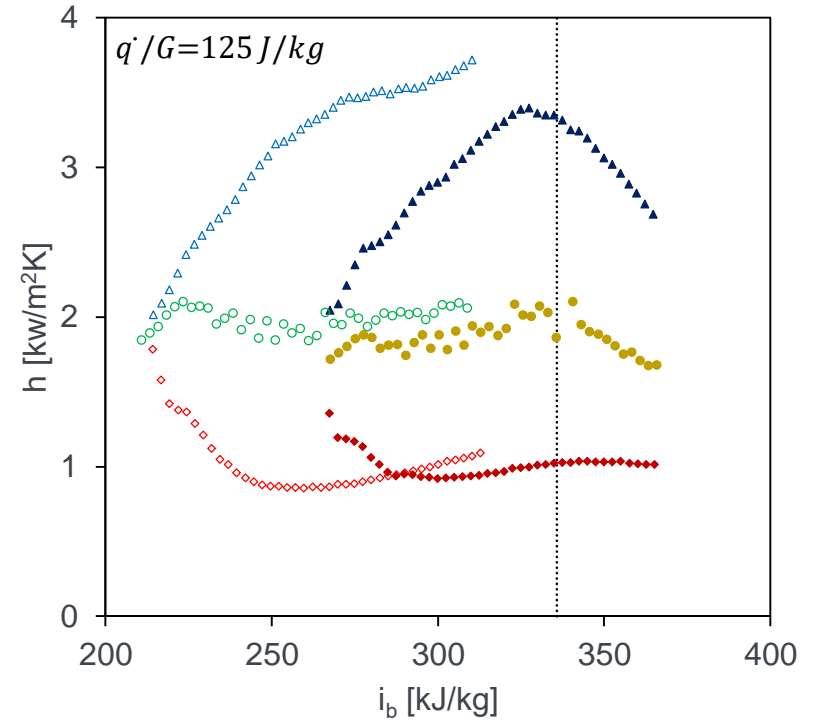
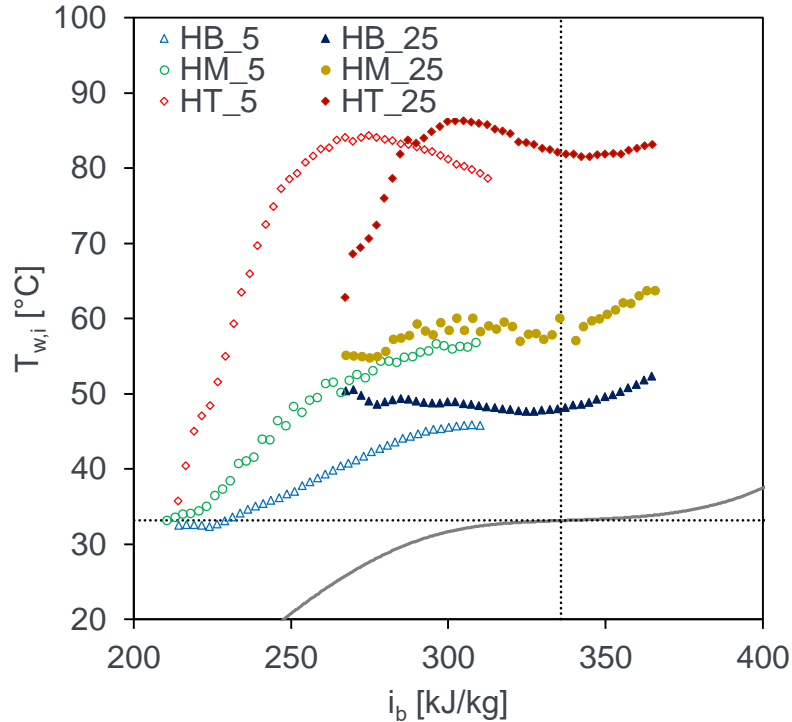
3rd test series – $d_i = 4 \text{ mm}$; $p = 7.75 \text{ MPa}$, $G = 800 \text{ kg/m}^2\text{s}$; $\dot{q} = 90 \text{ kW/m}^2$



- no clear temperature stratification
- temperature values converge after an enthalpy of approx. 430 kJ/kg

Results

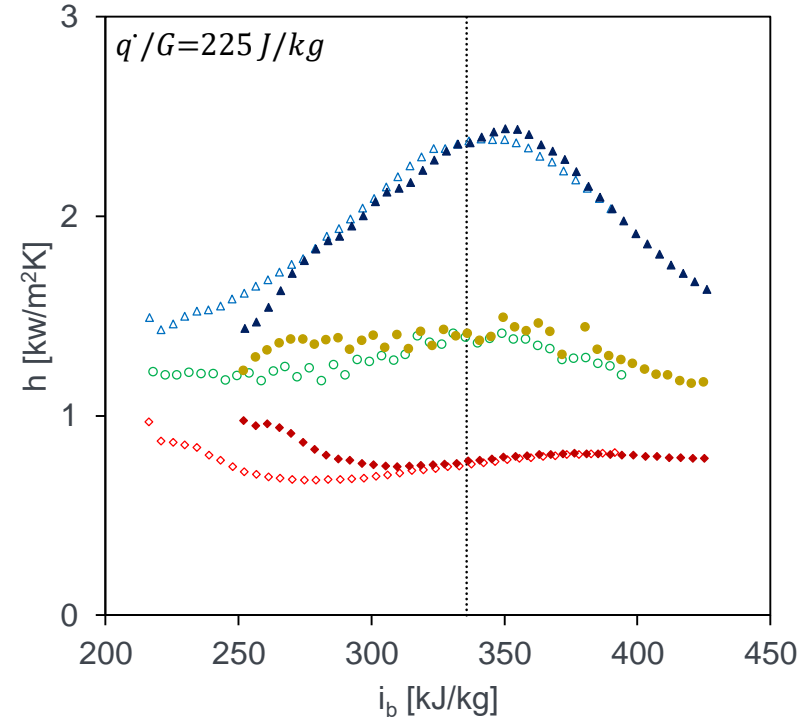
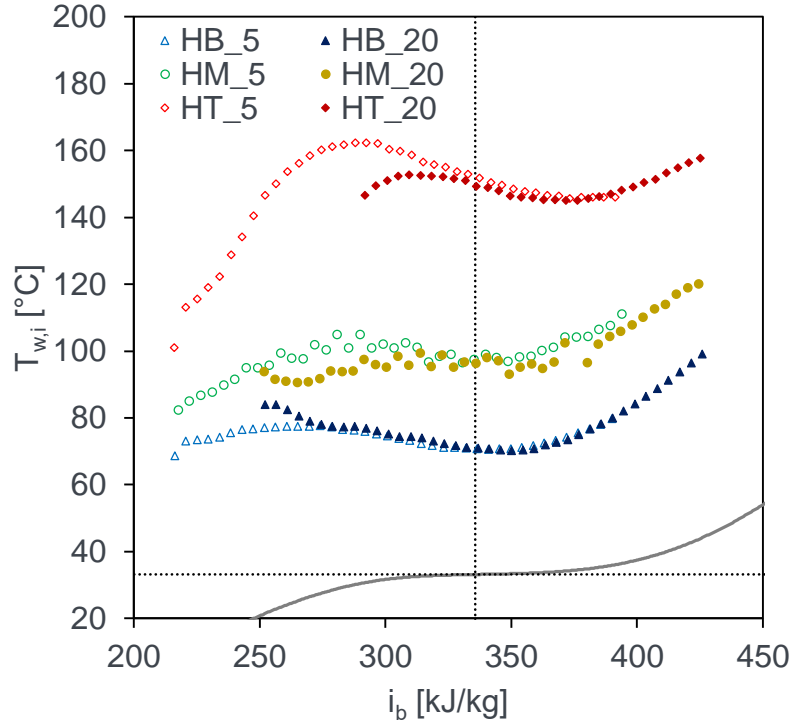
4th test series – $d_i = 8 \text{ mm}$; $p = 7.75 \text{ MPa}$, $G = 400 \text{ kg/m}^2\text{s}$; $\dot{q} = 50 \text{ kW/m}^2$



- stable temperature stratification (more pronounced than in the 1st test series)
- max. temperature difference between top and bottom surface approx. 45 K

Results

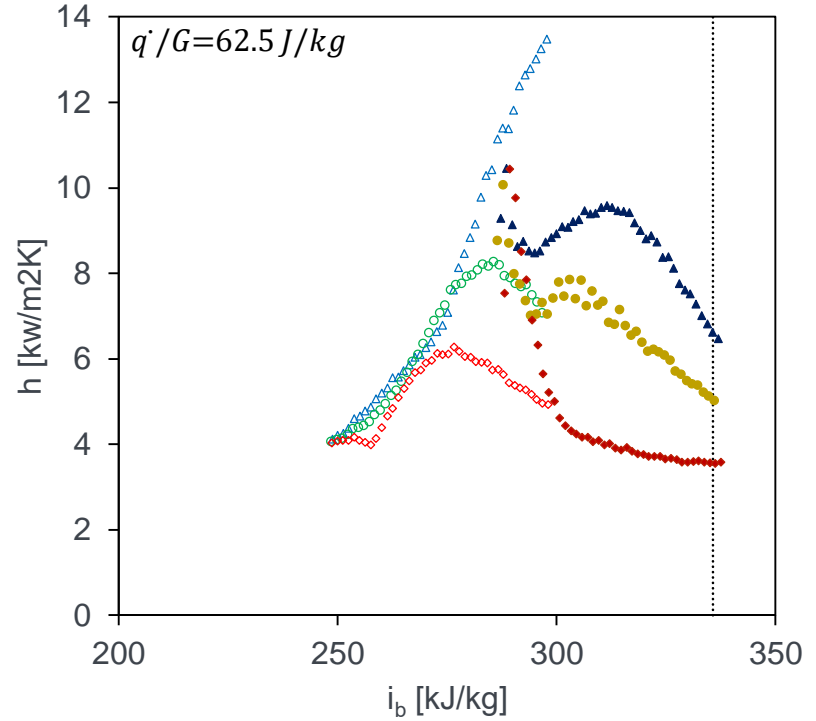
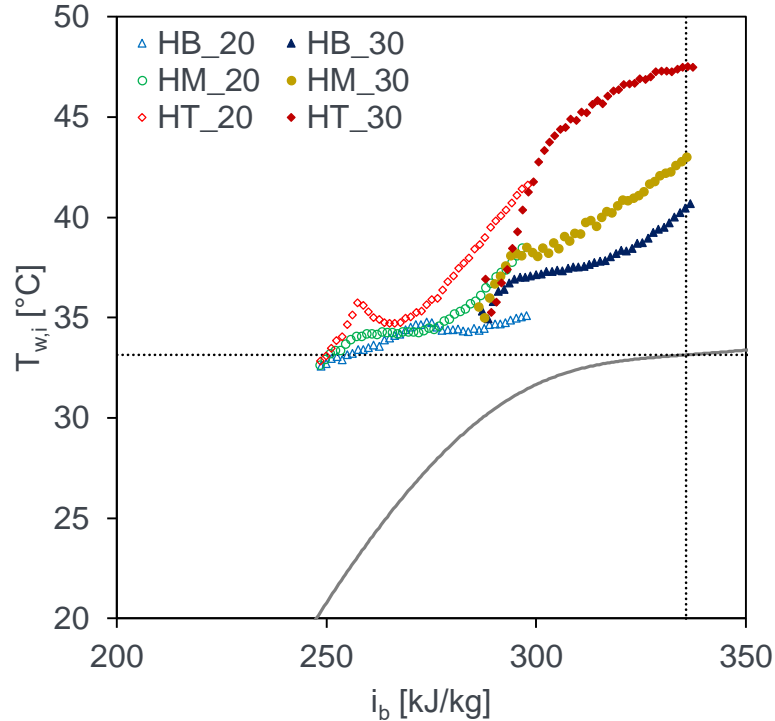
5th test series – $d_i = 8 \text{ mm}$; $p = 7.75 \text{ MPa}$, $G = 400 \text{ kg/m}^2\text{s}$; $\dot{q} = 90 \text{ kW/m}^2$



- stable temperature stratification (more pronounced than in the 4th test series)
- max. temperature difference between top and bottom surface approx. 90 K

Results

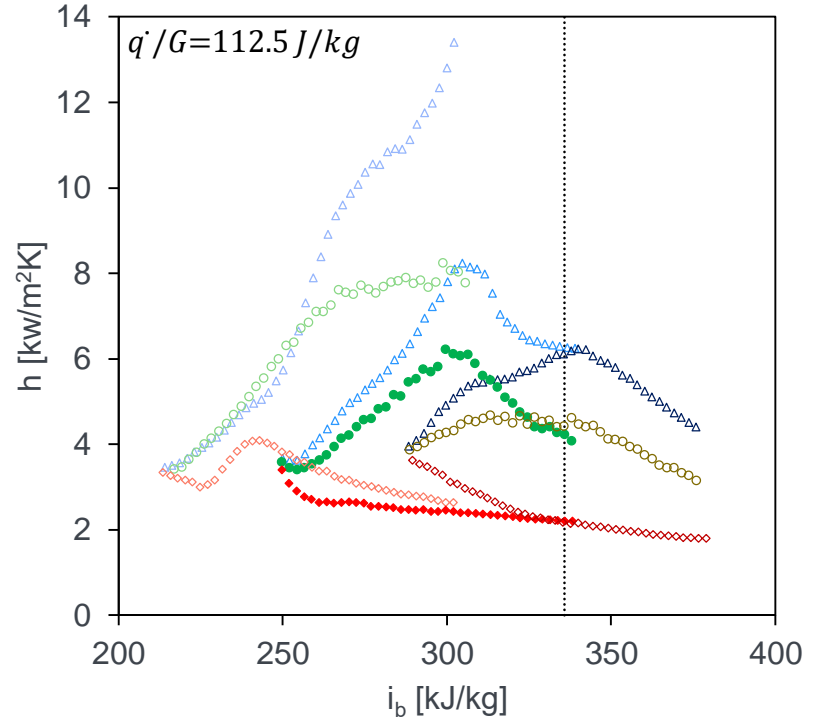
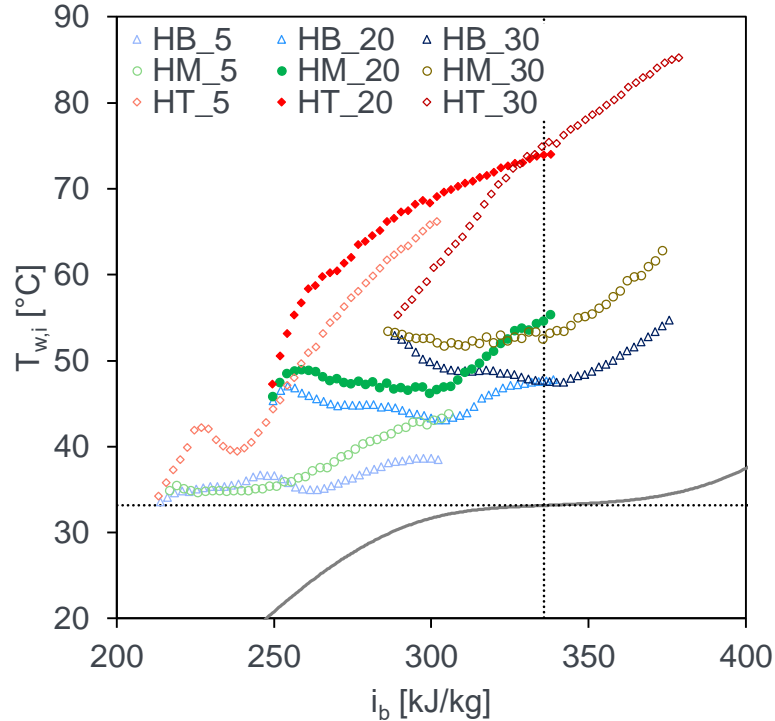
6th test series – $d_i = 8 \text{ mm}$; $p = 7.75 \text{ MPa}$, $G = 800 \text{ kg/m}^2\text{s}$; $\dot{q} = 50 \text{ kW/m}^2$



- stable temperature stratification (more pronounced than in the 2th test series)
- max. temperature difference between top and bottom surface approx. 7 K

Results

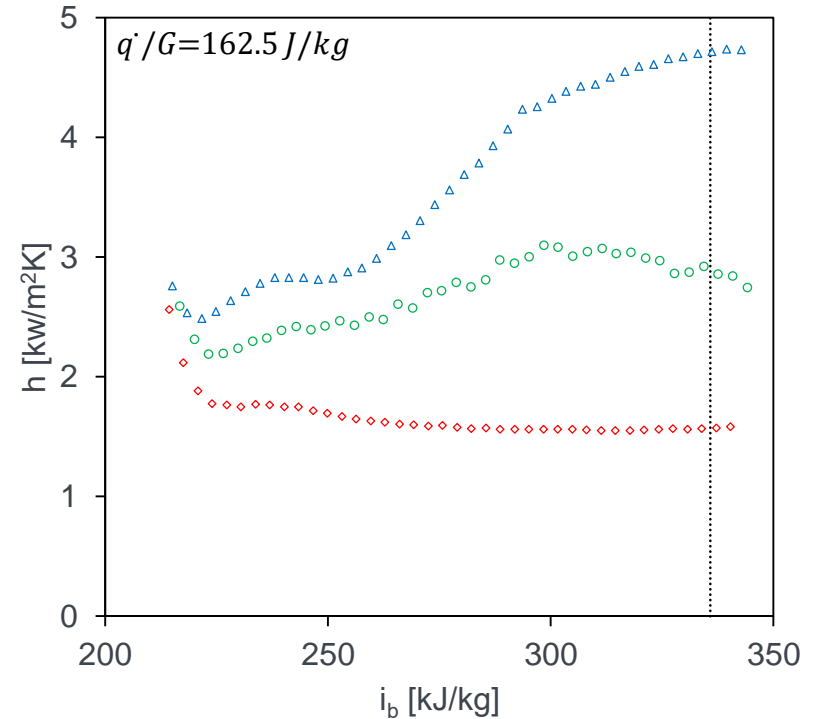
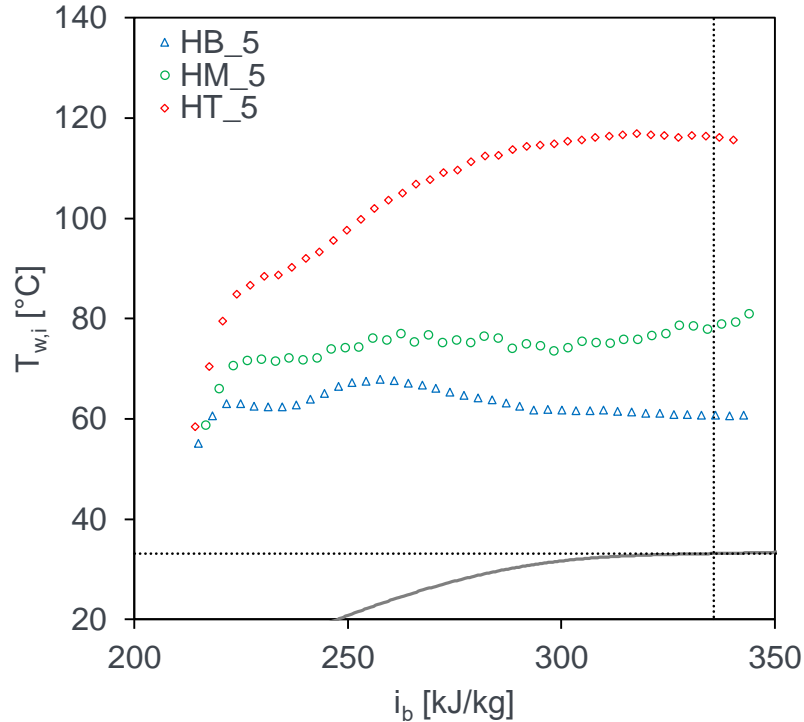
7th test series – $d_i = 8 \text{ mm}$; $p = 7.75 \text{ MPa}$, $G = 800 \text{ kg/m}^2\text{s}$; $\dot{q} = 90 \text{ kW/m}^2$



- with increasing heat flux the temperature stratification became much clearer
- max. temperature difference between top and bottom surface approx. 30 K

Results

8th test series – $d_i = 8 \text{ mm}$; $p = 7.75 \text{ MPa}$, $G = 800 \text{ kg/m}^2\text{s}$; $\dot{q} = 130 \text{ kW/m}^2$



- with increasing heat flux the temperature stratification became much clearer
- max. temperature difference between top and bottom surface approx. 60 K

Summery & Conclusion

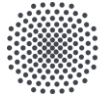
Eight test series with overall 48 experiments were carried out with 4 and 8 mm horizontal heated pipes.

- Heat transfer characteristics of sCO₂ were investigated in cases where buoyancy effects lead to a temperature stratification.
- The investigated cases show that...
 - ... increasing mass flux and Reynolds number at constant heat flux and inner diameter leads to reduced temperature differences between the top and bottom of the pipe.
 - ... no clear temperature stratification occurs by increasing the mass flux and the Reynolds number at constant heat to mass flux ratio and diameter.
 - ... at constant heat to mass flux ratio and Reynolds number, larger pipe diameters lead to more pronounced temperature stratification.

Acknowledgements



The presented work is funded by the German Federal Ministry for Economic Affairs and Energy (BMWi, project no. 1501557) on basis of a decision by the German Bundestag.



University of Stuttgart
Institute of Nuclear Technology
and Energy Systems

Thank you!



Konstantinos Theologou

e-mail konstantinos.theologou@ike.uni-stuttgart.de

phone +49 (0) 711 685-60786

fax +49 (0) 711 685-62010

University of Stuttgart
Institute of Nuclear Technology and Energy Systems
Pfaffenwaldring 31 • 70569 Stuttgart